Nuclear Instruments and Methods in Physics Research A310 (1991) 189–191
North-Holland

NUCLEAR INSTRUMENTS & METHODS IN PHYSICS RESEARCH
Section A

Electrostatic simulations for the design of silicon strip detectors and front-end electronics

R. Sonnenblick, N. Cartiglia, B. Hubbard, J. Leslie, H.F.-W. Sadrozinski and T. Schalk
Santa Cruz Institute for Particle Physics, University of California, Santa Cruz, CA 95064, USA

We report the first results from a simulation of the electrostatic properties of silicon microstrip detectors. We extract the capacitance and pulse shapes and show their importance for the design of front-end electronics and strip detector geometries for HERA and the SSC.

1. Motivation

In the past, the collection of charges in silicon strip detectors was usually treated as a static problem. When employing front-end electronics with typical integration time of the order 1 μs [1], the details of the charge collection proceeding in less than 50 ns was not critical, although one had to take into account secondary consequences of the charge transport in the detector, i.e., diffusion, and the Lorentz angle in a magnetic field [2]. With the advent of high luminosity colliders, shaping times become shorter and the motion of the electrons and holes have to be considered in the signal formation. The time between collisions will be 96 ns at HERA and 16 ns at the SSC, and the shaping time of the front-end electronics has to be commensurate to this time if one wants to identify the event bucket and minimize the dead time. In addition, the front end for silicon detectors at the SSC has to be low power and low noise at high speed. Circuit designs are constrained by the capacitance of the detectors which is dominated by the interstrip capacitance. Electrostatic calculations might allow one to optimize the detector design for small capacitance.

2. Simulations

Minimum ionizing particles create about 25000 electron–hole pairs in 300 μm detectors. The free charges in the bulk induce surface charges on the conductors. In the electric field created by the bias, the electrons and holes drift to opposite electrodes causing the induced charges to change, thus generating a current.

The basic equation for the induced current is [3]

$$i_{\mathrm{ind}} = -q\mu \boldsymbol{E}_{\mathrm{w}} \cdot \boldsymbol{E}_0,$$

where μ = mobility (assuming $v = \mu \boldsymbol{E}_0$), $\boldsymbol{E}_{\mathrm{w}}$ = weighting field (coupling between electrodes and charges located in the detector), and $\boldsymbol{E}_0$ = operating field (due to bias). The saturation of the drift velocity v near the strips is a noticeable effect for large bias voltages [4]. Note that i_{ind} is due both to electrons and holes on both the junction side (mainly holes) and on the ohmic side (mainly electrons). Also, given $\mu_e/\mu_h = 3$, the collection time of the electrons is three times shorter than for holes and the Lorentz angle of electrons is three times larger than for holes. In a typical microstrip detector, the strip length (10 cm) is orders of magnitude larger than either the thickness (300 μm) or the pitch (25–100 μm); hence the two-dimensional Poisson equation is sufficient to calculate $\boldsymbol{E}_0$ and $\boldsymbol{E}_{\mathrm{w}}$. In order to calculate the two fields, we used a finite difference approximation on a 1 μm square grid and let the potential map relax, using fixed voltages as boundary conditions.

3. Capacitance

The capacitance of the strip detector is calculated integrating the weighting field $\boldsymbol{E}_{\mathrm{w}}$ over the electrodes. It is proportional to the strip length and for the geometries considered is dominated by interstrip capacitance. It depends on the ratio of strip width to strip pitch. Fig. 1 shows the calculated capacity per length as a function of the ratio x = width/pitch for different detector pitches. These simulations can be compared to measurements. Using an HP 4284 LCR meter we have measured the strip capacity of two different strip detectors. For an 8.2 cm long detector with 29 μm pitch and 8 μm implant width ($x = 0.276$) we measured 1.47 pF/cm, and for a 5.2 cm long detector with 81 μm pitch and 30 μm implant width ($x = 0.37$) we measured

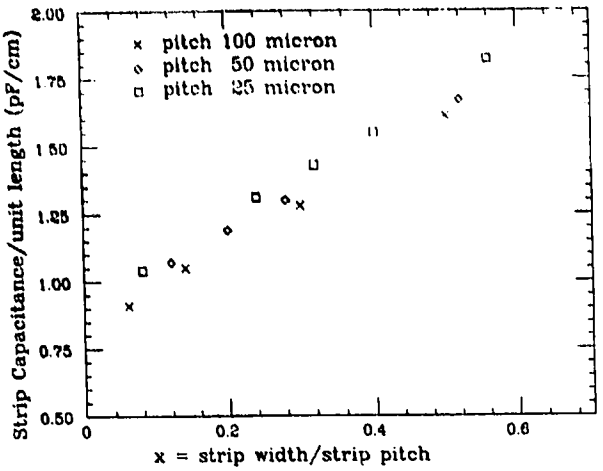

Fig. 1. Capacity per unit length for strip detectors of different pitch as function of the ratio x of implant width to strip pitch.

1.38 pF/cm. Using the equivalent noise charge in a preamplifier, Adolphsen et al. [5], have measured the capacitance of a 7.2 cm long detector with 25 μm pitch and $x = 0.32$ to be 1.39 pF/cm. All these results agree within 15% of the prediction in fig. 1. The minimum capacitance occurs for the smallest implant width. It would be interesting to investigate how much either the implant width or the implant depth can be minimized in the manufacturing process.

4. Pulse shape

We have calculated induced currents due to traversing minimum ionizing particles using the numerically calculated weighting and operating fields and have compared them with measurements of pulse shapes on single-sided detectors where the collection occurs on the junction side. (The extension of the simulation to the ohmic side where the electrons are collected in about one third of the time is straightforward.) We begin with 25000 electron–hole pairs uniformly distributed along the particle path and then determine the induced current due to their drift and diffusion. A radial, ambipolar diffusion – with no drift – occurs until the density of electron–hole pairs reaches N_D, the doping concentration [6]. This effect is only of small experimental consequence for minimum ionizing particles, but for highly ionizing particles such as α's the effect will contribute significantly to the pulse shape. For the detector described below, fig. 2a shows the current induced by the electrons, the holes, and both combined, assuming no diffusion. Fig. 2b shows the same, assuming, however, ambipolar diffusion in the high density regions and drift and lateral diffusion in low density regions. We have measured the pulse shape due to minimum ionizing electrons from a ^{106}Ru source with a HP 5411D digitizing scope, using a ultra low-noise amplifier of 100 MHz bandwidth [7] connected to microstrip detectors of 25 μm pitch and 300 μm thickness. The detector depleted at 55 V and we biased it at 100 V. We have convoluted the simulated pulse with the amplifier response function $\lambda e^{-t\lambda}$ where $1/\lambda = 3$ ns and using a transresistance of $R = 4$ kΩ. Fig. 3 shows the nonconvoluted pulse shape (from fig. 2b), the convoluted pulse shape, and a typical measured pulse. The agreement between simulation and measurement is good both in shape and absolute value. This agreement encourages us to use the simulation program to predict efficiencies, position resolution, the response of different front-end designs and the consequence of radiation damage. For example we have started to investigate how the shaping time of the pre-amplifier affects what fraction of the deposited electron–hole pairs contribute to the signal pulse within the peaking time. A similar analysis was performed by Sailor et al. [8], who used an analytic solution for the pulse form.

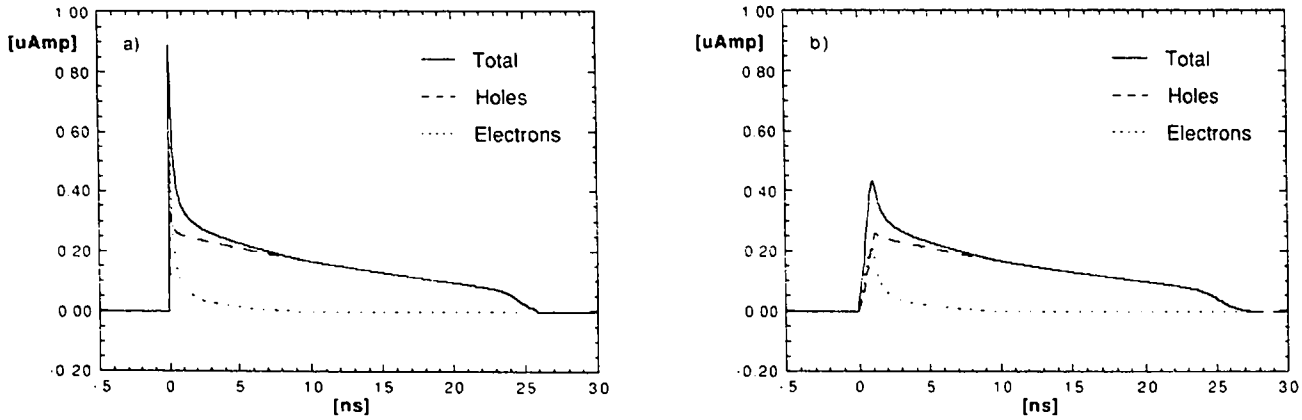

Fig. 2. Current pulse generated at the junction side from a minimum ionizing particle. The strip pitch is 25 μm and the implant width 8 μm. (a) The generated current for electrons, holes and both respectively. (b) Same as (a) but including the diffusion. Amplifier response with finite shaping times will eliminate the difference between the two cases.

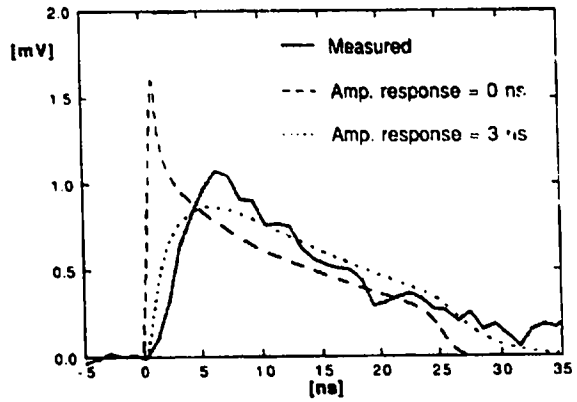

Fig. 3. Pulse shape at the junction side from a minimum ionizing particle. The three curves are the simulated current (with initial diffusion), the simulated current convoluted with the preamplifier response, and a typical observed pulse, respectively.

5. Conclusions

- The use of silicon strip detectors enters a new phase where the details of the charge transport becomes important.
- We have found agreement between simulated and measured pulse shapes. Simulations will be used to evaluate efficiencies, time and position resolution as function of the predicted signal/noise ratio, and consequences of radiation damage.
- We will explore the parameter space of the strip detectors to build low-capacitance detectors in order to be able to use low-power and low-noise front ends at high speed.

References

[1] C. Adolphsen et al., IEEE Trans. Nucl. Sci. NS-35 (1988) 424.
[2] E. Belau et al., Nucl. Instr. and Meth. 214 (1983) 253.
[3] S. Ramo, Proc. IRE 27 (1939) 584;
E. Gatti and P.F. Manfredi, Rev. Nuovo Cimento 9 (1986) 1;
V. Radeka, Ann. Rev. Nucl. Part. Sci. 38 (1988) 217;
P.M. Morse and H. Feshbach, Methods of Theoretical Physics (McGraw-Hill, 1953) 1176.
[4] S.M. Sze, Physics of Semiconductor Devices (Wiley, New York, 1981) 44.
[5] C. Adolphsen, private communication and ref. [1].
[6] G.C. Messenger, IEEE Trans. Nucl. Sci. NS-29 (1982) 6.
[7] E. Gottlieb, Senior Thesis, University of California, Santa Cruz Board of Studies in Physics (1990).
[8] W.C. Sailor, H.J. Ziock, W.W. Kinnison and K. Holzscheiter, Nucl. Instr. and Meth. A303 (1991) 285.